

## Canonical decomposition of ictal scalp EEG reliably detects the seizure onset zone

M. De Vos,<sup>a,\*</sup> A. Vergult,<sup>a</sup> L. De Lathauwer,<sup>b</sup> W. De Clercq,<sup>a</sup> S. Van Huffel,<sup>a</sup>  
P. Dupont,<sup>c</sup> A. Palmi,<sup>d</sup> and W. Van Paesschen<sup>d</sup>

<sup>a</sup>Katholieke Universiteit Leuven, Department of Electrical Engineering, Leuven, Belgium

<sup>b</sup>CNRS-ETIS, Cergy-Pontoise, France

<sup>c</sup>University Hospital Gasthuisberg, Department of Nuclear Medicine, Leuven, Belgium

<sup>d</sup>University Hospital Gasthuisberg, Department of Neurology, Leuven, Belgium

Received 9 November 2006; revised 6 April 2007; accepted 19 April 2007

Available online 21 May 2007

**Long-term electroencephalographic (EEG) recordings are important in the presurgical evaluation of refractory partial epilepsy for the delineation of the irritative and ictal onset zones. In this paper we introduce a new algorithm for an automatic, fast and objective localizing of the ictal onset zone in ictal EEG recordings. We extracted the potential distribution of the ictal activity from EEG using the higher order canonical decomposition method, also referred to as the CP model. The CP model decomposes in a unique way a higher order tensor in a minimal sum of rank-1 ‘atoms’. We showed that only one atom is related to the seizure activity. Simulation experiments demonstrated that the method correctly extracted the potential distribution of the ictal activity even with low signal-to-noise ratios. In 37 ictal EEGs, the CP method correctly localized the seizure onset zone in 34 (92%) and visual assessment in 21 cases (57%) ( $p=0.00024$ ). The CP method is a fast method to delineate the ictal onset zone in ictal EEGs and is more sensitive than visual interpretation of the ictal EEGs.**

© 2007 Elsevier Inc. All rights reserved.

### Introduction

The objective of epilepsy surgery is the complete resection of the epileptogenic area, i.e., the region of the cortex that has to be removed in order to make the patient seizure-free. In order to pinpoint the epileptogenic area during a presurgical evaluation, a variety of diagnostic methods is available. Most often, this localization is based on the combination of clinical ictal symptoms and signs on video recordings of seizures, MRI-visible epileptic lesions, regions of hyperperfusion on ictal SPECT and interictal

and ictal epileptic activity on EEG recordings (Rosenow and Lüders, 2001).

The ictal EEG gives time information about the voltage distribution over the electrodes on the scalp during a seizure and is the most commonly used method to localize the ictal onset zone (Foldvary et al., 2001). Interrater variability in the visual interpretation of ictal scalp EEG recordings is considerable, and seizure activity is often obscured by muscle and other artifacts (Spencer et al., 1985). The sensitivity of ictal EEG to localize the seizure onset zone is only 40–70% (Foldvary et al., 2001), which can be improved by removal of artifacts with different techniques (Urrestarazu et al., 2004; Delorme et al., 2007; and references herein). Nowadays, muscle artifacts can be removed using the BSS-CCA method (De Clercq et al., 2006; Vergult et al., 2007). However, BSS-CCA is only a semi-automatic preprocessing method to remove muscle artifacts, and subjective visual assessment is still required for a correct interpretation and localization of the ictal onset zone.

A more objective way than visual analysis to estimate the epileptogenic focus is EEG dipole source localization (Scherg and von Cramon, 1985). Dipole modeling is a well-established technique for localizing interictal spikes and the irritative zone (Kobayashi et al., 2005). Dipole modeling of ictal EEG activity has been more difficult mainly due to EEG artifacts often seen during seizures (Gotman, 2003).

Our aim was to establish a robust and automatic localization method for ictal EEG activity, using the canonical decomposition (CANDECOMP), also known as parallel factor analysis (PARAFAC), often referred to as the CP (CANDECOMP/PARAFAC) decomposition. With this decomposition, multichannel time-varying EEG is decomposed into a series of distinct ‘atoms’, which represent in an ideal situation distinct brain sources. The CP decomposition can be considered as the higher order variant of factor analysis. The aim of factor analysis is to relate the different ‘atoms’ to the different ‘physical mechanisms’. However, it is never a priori known whether an atom obtained with factor analysis

\* Corresponding author.

E-mail address: maarten.devos@esat.kuleuven.be (M. De Vos).

Available online on ScienceDirect (www.sciencedirect.com).

truly reveals the underlying phenomenon. Factor analysis of matrices is underdetermined, and assumptions like orthogonality or independence, which may be irrelevant, have to be imposed in order to obtain a ‘unique’ solution. Factor analysis of higher order data sets is unique under mild conditions. We will show that the CP decomposition reliably identifies one epileptical seizure onset atom.

Atomic decompositions of the EEG in matrix form have been shown to be useful as an exploratory tool. With principal component analysis (PCA) and independent component analysis (ICA), space–time decompositions of multichannel EEG can be used for artifact removal (e.g. Urrestarazu et al., 2004; LeVan et al., 2006) or for extracting interesting activities (e.g. Tang et al., 2004). The CP model was used for the simultaneous space–time–frequency decomposition of the power of wavelet transformed EEG with dimensions channels×time×scales (Miwakechi et al., 2004). It was shown that the CP allowed identifying frontal theta atoms during a cognitive task and occipital alfa atoms during resting conditions. In Morup et al. (2006), CP was used as an exploratory tool in the analysis of inter-trial phase coherence of event-related EEG. Another tensor decomposition, the Tucker model, does not give an atomic decomposition, but it is recently used for seizure analysis (Acar et al., 2006). Separation of the ictal source into one component has not been reported.

Ictal seizure activity is known to consist of rhythmical waves often with a frequency between 3 and 29 Hz (Gotman, 1982). As the CP decomposition of wavelet transformed EEG is especially useful in the description of oscillatory phenomena, the goal of this study was to investigate the localizing value of the epileptical atom, identified after CP decomposition. In contrast to previous studies, where the CP decomposition was computed on the power of wavelet transformed EEG, we computed the decomposition on the ‘pure’ wavelet transform of the ongoing EEG recording, which made the decomposition more robust with respect to artifacts. We assessed the accuracy of this method with a realistic simulation study. Finally, we validated our method clinically on a set of ictal EEG recordings and showed that the CP method was more sensitive than visual interpretation of the ictal EEGs in localizing the ictal onset zone.

**Methods and materials**

We define the three-way data array as the wavelet transform of the ongoing EEG recording, introduce the CP decomposition as a multilinear generalization of the matrix singular value decomposition (SVD) and describe how the CP decomposition can be used for seizure onset localization.

*Wavelet transform*

Fourier transform (FT) of EEG data can estimate the frequency content of the signal (Dietsch, 1932) but does not reveal time-varying frequency changes in the signal. Even the short-time Fourier analysis (STFA) is an inaccurate and inefficient method of time–frequency localization because the interval in which the frequency content is computed is fixed. Since the time and frequency resolutions are reciprocal, good time resolution means poor frequency resolution and vice versa. Optimal time–frequency analysis is given by the wavelet transform. Wavelets resolve high-frequency components within small time windows and low

frequencies in larger time windows. The continuous wavelet  $C$  at scale  $a$  and time  $t$  of a signal  $x(t)$  is defined by

$$C(a, \text{time}) = \int_{-\alpha}^{\alpha} x(t)\phi(a, \text{time}, t)dt$$

with  $\phi$  the chosen wavelet. We used in this study a biorthogonal wavelet with decomposition order 3. The exact choice of the wavelet does not really affect the result in our study as long as a real wavelet is chosen. From the scale  $a$  of the wavelet, the frequency  $f$  of the signal can be estimated as:

$$f = \frac{f_c}{a\Delta t}$$

with  $f_c$  the center frequency of the wavelet and  $\Delta t$  the sampling period.

*CP decomposition as a higher -order generalization of the matrix SVD*

A two-way array can be decomposed by means of an SVD. There are several ways to generalize the SVD to higher orders: the Tucker models (Tucker, 1964, 1966), the higher order SVD (De Lathauwer et al., 2000) and the CP decomposition (Hitchcock, 1927; Harshman, 1970; Carroll and Chang, 1970; De Lathauwer, 2006). The main success of the CP model is due to its uniqueness and related interpretability of the components. We will introduce this concept as a generalization of the SVD.

Given a matrix  $\mathbf{X}^{(I \times J)}$ . Based on its SVD,  $\mathbf{X} = \mathbf{A} \mathbf{\Sigma} \mathbf{B}^T$  truncated to  $R$  components, the elements  $x_{ij}$  can be written as:

$$x_{ij} = \sum_{r=1}^R s_{rr} s_{ir} b_{jr} + e_{ij}$$

where the matrices  $\mathbf{A}^{(I \times R)}$  (with elements  $a_{ij}$ ) and  $\mathbf{B}^{(J \times R)}$  (with elements  $b_{ij}$ ) are both orthonormal matrices.  $\mathbf{\Sigma} = \text{diag}(s_{11}, \dots, s_{rr})$  is a diagonal matrix containing the  $R$  largest singular values of  $\mathbf{X}$ , and  $e_{ij}$  is the residual. The values of  $s_{rr}$  can also be absorbed in one mode, leading to the model

$$x_{ij} = \sum_{r=1}^R a_{ir} b_{jr} + e_{ij}$$

The SVD restricted to  $R$  atoms is visualized in Fig. 1.

The generalization of the SVD to the trilinear CP model for a three-way array  $\mathbf{X}^{(I \times J \times K)}$  given by:

$$x_{ijk} = \sum_{r=1}^R a_{ir} b_{jr} c_{kr} + e_{ijk}$$

where  $R$  is the number of components used in the CP model and  $e_{ijk}$  is the residual containing the unexplained variation. A pictorial

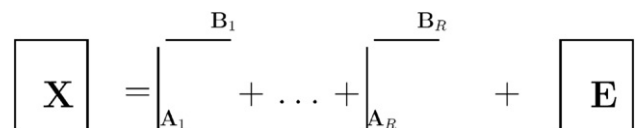


Fig. 1. The singular value decomposition restricted to  $R$  atoms.

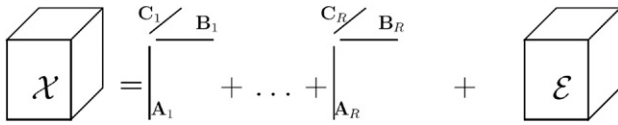


Fig. 2. The CP decomposition with  $R$  atoms.

representation of the CP decomposition with  $R$  atoms is given in Fig. 2.

The CP model is a trilinear model: fixing the parameters in two modes,  $x_{ijk}$  is expressed as a linear function of the remaining parameters. A difference with the SVD is that the components of a CP model do not have to be orthogonal with respect to each other. Another equivalent and useful expression of the same CP model is given in terms of the Khatri–Rao product  $\odot$  (Smilde et al., 2004).

Stack the elements of the tensor  $\mathbf{X}^{(I \times J \times K)}$  in a matrix  $\mathbf{X}^{(I \times J \times K)}$  as follows:

$$\mathbf{X}_{(i-1)J+j,k} = x_{ijk}$$

A matrix  $\mathbf{E}$  is formed in a similar way. Collect the elements  $a_{ir}$  in  $\mathbf{A}$ ,  $b_{jr}$  in  $\mathbf{B}$  and  $c_{kr}$  in  $\mathbf{C}$ . Then

$$\mathbf{X}^{I \times J \times K} = (\mathbf{X}^{I \times R} \odot \mathbf{B}^{J \times R})(\mathbf{C}^{K \times R})^T + \mathbf{E}^{I \times J \times K}$$

Comparing the number of free parameters of a generic tensor and a CP model, it can be seen that this model is very restricted. For example, a random third order tensor of dimensions  $(I \times J \times K)$  has  $I \cdot J \cdot K$  elements, whereas a third-order rank- $R$  CP decomposition has only  $R \cdot (I + J + K)$  elements. The advantage of this model is its uniqueness under mild conditions (Sidiropoulos and Bro, 2000; Kruskal, 1977; Stegeman and Sidiropoulos, 2007):

$$k_{\mathbf{A}} + k_{\mathbf{B}} + k_{\mathbf{C}} \geq 2R + 2$$

with  $k_{\mathbf{M}}$  the  $k$ -rank of matrix  $\mathbf{M}$ . Another, less restrictive uniqueness condition was recently derived in (De Lathauwer, 2006).

The CP decomposition is usually computed by means of an alternating least squares (ALS) algorithm (Smilde et al., 2004). This means that the least squares cost function

$$f(\mathbf{A}, \mathbf{B}, \mathbf{C}) = \|\mathbf{X} - \sum_{r=1}^R \mathbf{A}_r \cdot \mathbf{B}_r \cdot \mathbf{C}_r\|^2$$

is minimized by means of alternating updates of one of its matrix arguments, keeping the other two matrices fixed. Because the CP decomposition is a multi-linear decomposition, each update just amounts to solving a classical linear least squares problem. The convergence may be local. To increase the probability that the global minimum is found, the algorithm may be reinitialized a couple of times. Afterwards, other computational schemes are proposed (De Lathauwer et al., 2004; De Lathauwer, 2006).

#### Standardization

Before computing the CP decomposition, the data have to be carefully preprocessed. Standardization of the EEG was done by centering (i.e. subtracting the mean) the original EEG and dividing each channel by its standard deviation. After the decomposition, the spatial distribution of the scalp potential was again multiplied

with this standard deviation in order to conserve the amplitude information.

#### CP decomposition for seizure localization

After wavelet transformation of every channel of the original EEG at the seizure onset with dimensions (channels  $\times$  time), a three-way array with dimensions (channels  $\times$  time  $\times$  scales) was obtained. We chose 2 s as length of the time window as an optimal trade-off. A smaller time window will give a less stable decomposition. A larger time window would enlarge the risk that the seizure activity is already propagating in a realistic setting or to include eye blink artifacts (see for example Fig. 7). The seizure onset was defined as the time point when an ictal EEG discharge was observed without going back in time. It should be stressed that it is sufficient that a neurophysiologist is able to observe an ictal EEG change, even if the neurophysiologist is not able to localize the ictal onset zone at that point in time (e.g. generalized attenuation of EEG signal, ictal EEG changes obscured by muscle artifact, etc.). This three-way array was decomposed with a CP model. There are several ways of determining the correct number of atoms (Smilde et al., 2004). By checking the core consistency diagnostic, we found that the optimal number of atoms was two ( $R=2$ ).

When the goal is to localize the seizure onset region, the seizure atom has to be identified after the decomposition. We identified the epileptic atom by ordering of the atoms. The atoms in a CP decomposition are not ordered by the decomposition as it is the case with the SVD. We put all the variance of an atom into the spatial mode and ordered the components according to their contribution. The atom with the highest contribution contained the ictal activity provided that no eye blinks were present and the EEG was first standardized, as described. The spatial component of the identified atom gave the spatial distribution of the epileptic activity. The electrodes with a resulting potential above a predefined threshold (we used 75% of the maximal value of amplitudes across all channels for fixed atom) defined the epileptic focus. In addition, it was verified that the maximal frequency of the frequency distribution corresponded to the frequency of the rhythmical seizure activity.

The CP decomposition of a pure wavelet transformed ictal EEG is illustrated in Fig. 3.

#### Simulation study

Consider a matrix  $\mathbf{X}$  of dimension  $500 \times 21$  representing a 21-channel EEG section of 2.0 s long. Each vector  $\mathbf{x}_s$ ,  $s=1, \dots, 21$  of  $\mathbf{X}$  contains the time course of an EEG channel:

$$\mathbf{X} = [\mathbf{x}_1, \mathbf{x}_2, \dots, \mathbf{x}_{21}]^T$$

In this simulation study,  $\mathbf{X}$  includes both seizure activity and superimposed noise. Both signals are described below.

The EEG of the ictal activity (Fig. 4A) was generated using a fixed dipole in a three-shell spherical head model with a moment having a 5.7-Hz sinusoidal waveform (for example, typical in patients with mesial temporal lobe epilepsy (MTLE); Niedermeyer, 1987) (Fig. 4A). The amplification factors at each electrode were computed by solving the forward problem for a dipole in a three-shell spherical head model consisting of a brain, a skull and a scalp compartment (Salu et al., 1990). Each compartment had a specific conductivity with a ratio equal to 1:1/16:1 for the brain, skull and

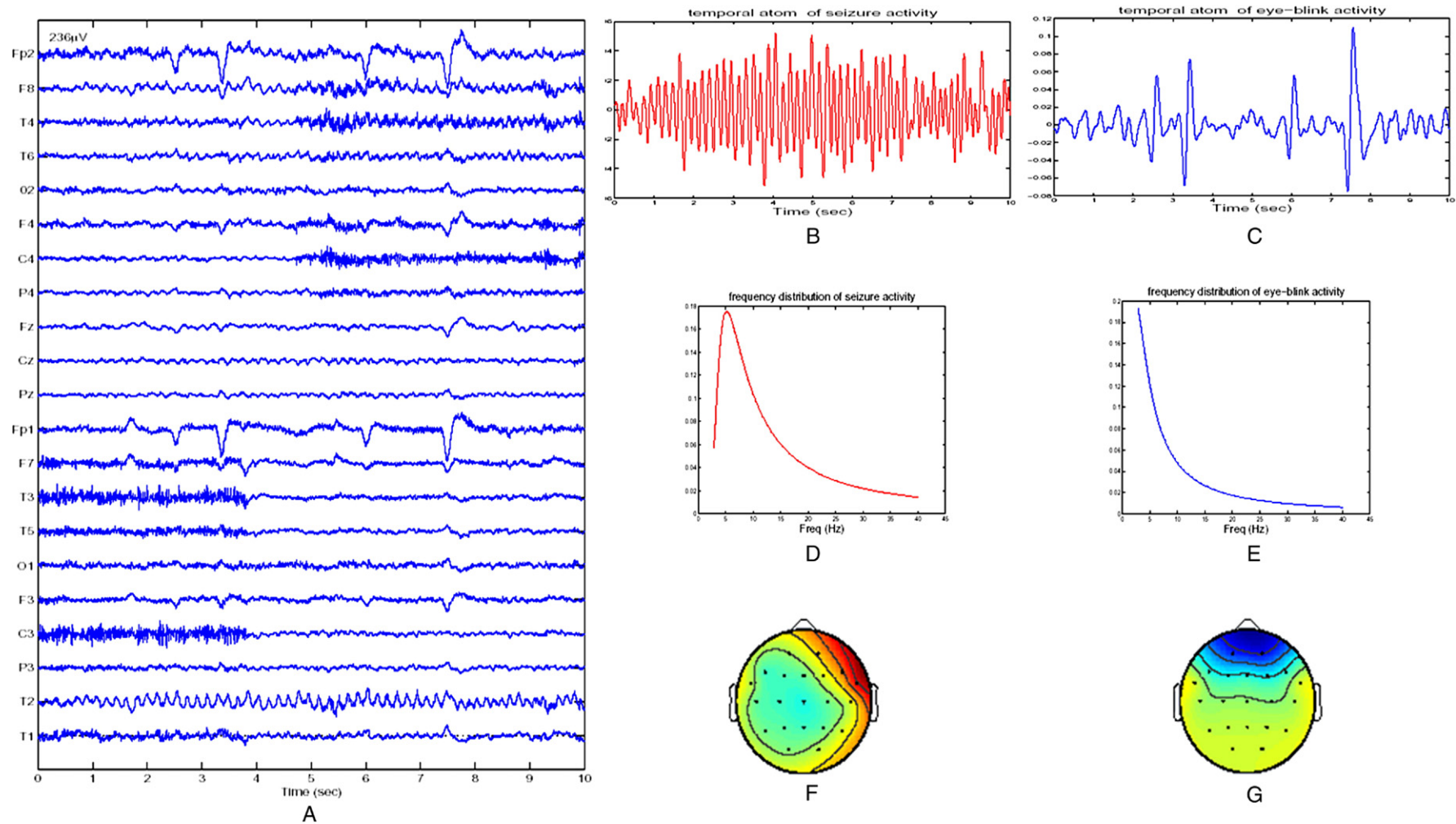


Fig. 3. CP decomposition of a pure wavelet transformed ictal EEG. A 21-channel average reference montage EEG showed 10 s of the beginning of a right temporal lobe complex partial seizure, characterized by a recruiting theta rhythm of around 5 Hz over the right temporal derivations (T2 (sphenoidal electrode), F8, T4, and also T6) (A). There were muscle (e.g. first 3 s in T3 and C3, and last 5 s in C4) and eye blink artifacts (FP1 and FP2, asterisks). The EEG data matrix was wavelet transformed to obtain a 3D tensor without any artifact removal. The three modes of the CP decomposition of the 10 s of ictal EEG are shown: temporal mode (B and C), frequency mode (D and E) and spatial mode (F and G). The blue atom (C, E, G) was related to the eye blink artifacts. The temporal mode (C) showed high peaks at the same time of the eye blinks in the original EEG (asterisks in A). The frequency mode (E) showed a peak at low frequencies, consistent with low-frequency eye blinks. The spatial component (G) showed the typical distribution of eye blinks at FP1 and FP2. The red atom (B, D, F) contained all the information related to the ictal activity. The temporal mode (B) reflected the rhythmicity of the ictal wave. The frequency mode (D) displayed a peak at around 5.7 Hz, which corresponded to the frequency of the recruiting theta waves in the ictal EEG (A). The spatial mode (F) showed that the potential distribution of the ictal activity had maximal values (red area) in the antero- and midtemporal and sphenoidal electrodes of the right temporal lobe, which was also readily apparent on visual inspection of the ictal EEG (A). Notice that the spatial mode (F and G) is a two-dimensional display, with the right side corresponding to the right side of the patient, and the black dots representing the electrode positions according to the 10–20 system. Red regions indicated highly positive potentials, dark blue regions indicate highly negative potentials.

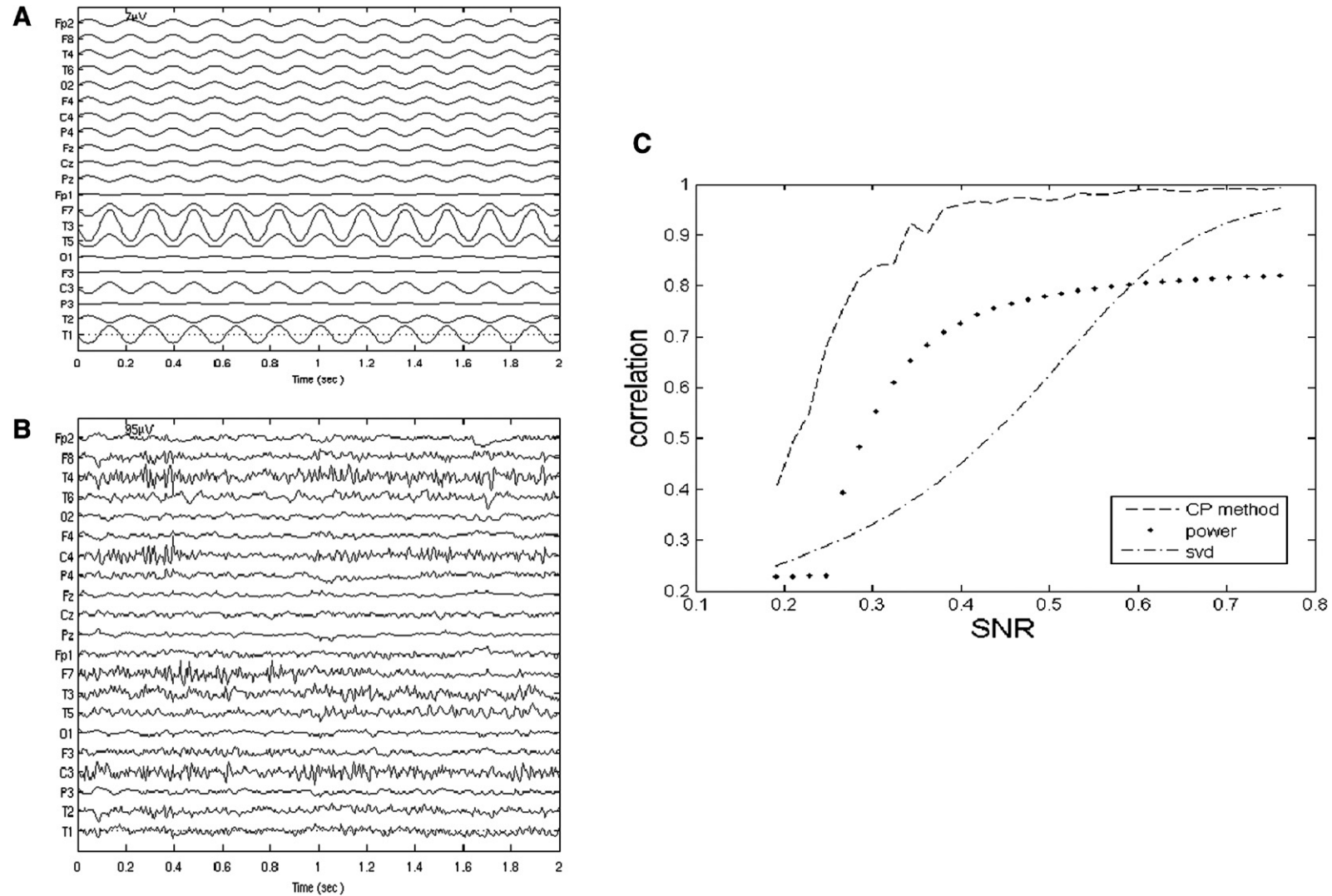


Fig. 4. Simulated data. Noise-free simulated ictal activity (A). The 2-s time course of the scalp potentials showed 5.7-Hz rhythmic activity in all electrodes with highest amplitude at T3 and T1. A simulated data matrix was obtained by mixing the noise-free simulated ictal activity (A) with noise resembling muscle artifact. In the example of (B), the SNR was equal to 0.42. The correlation between the simulated distribution and the spatial distribution, extracted with the CP method, is shown in panel C. The 5.7-Hz seizure activity was largely embedded in noise. The correlation for wavelet transformed EEG remained high up to an SNR of around 0.3. At an SNR of 0.42 in panel B, the correlation was 0.98, which means that the correct spatial distribution of the seizure activity was obtained with the CP decomposition, i.e. the method appeared insensitive to noise resembling muscle artifact. Also notice that the performance of the CP method for power of wavelet transformed EEG data was worse, compared with wavelet transformed EEG signals. Panel C also shows the correlation between the simulated distribution and the spatial distribution, extracted with the CP method and with the SVD on the same simulated data. Introducing the third, frequency dimension clearly improves the localization.

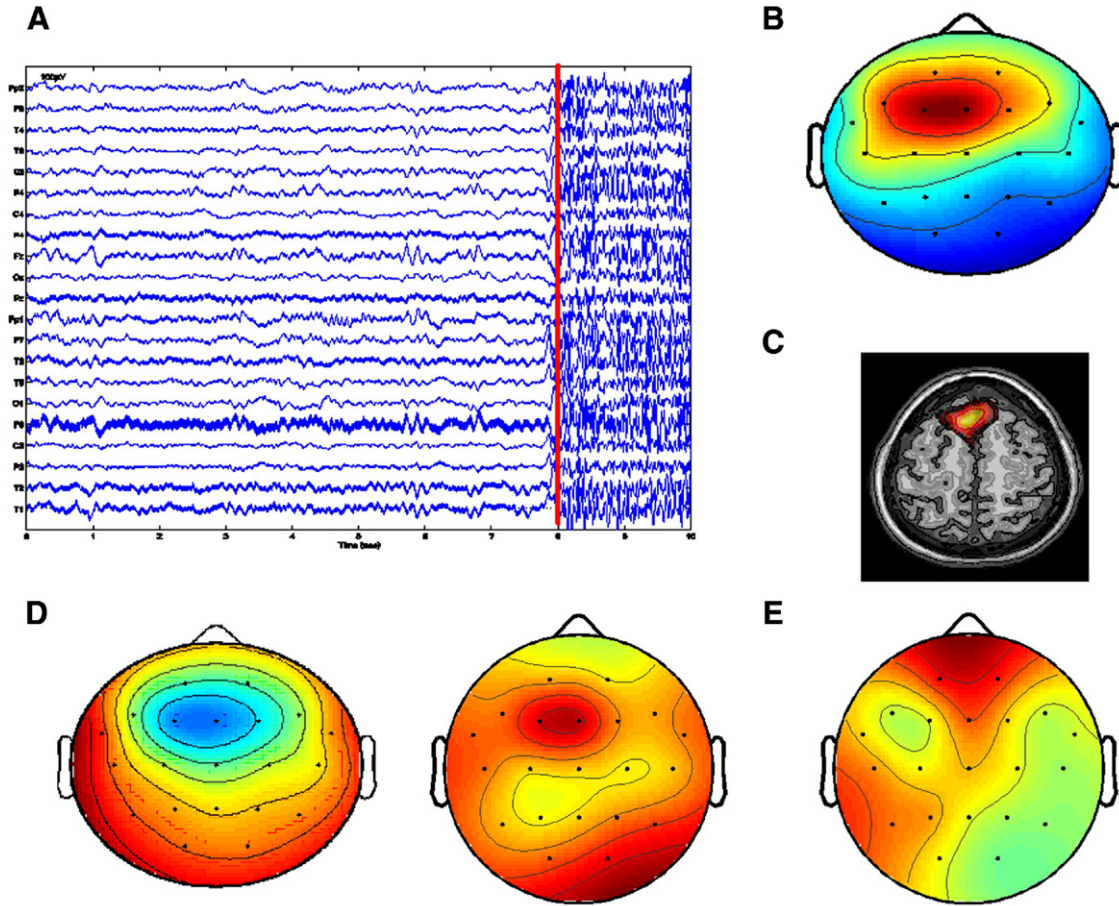


Fig. 5. (A) 10-s EEG recording of a left frontal lobe seizure, the red line indicates the start of the 2-s used in the CP analysis. (B) The spatial distribution of the epileptical atom (red area) and (C) SISCOM. The ictal EEG (last 2-s) was severely contaminated by muscle artifacts, and localization by visual assessment was impossible. The CP method, however, showed a potential distribution concordant with SISCOM. (D) The first singular vector did not give clear localizing information. (E1–2) Spatial distributions of the 2 atoms of the decomposition of the power of wavelet transformed EEG did not reveal the epileptic focus.

scalp compartment, respectively (Oostendorp et al., 2000). The brain and scalp conductivity was  $3.3 \cdot 10^{-4} / \Omega / \text{mm}$  (Cuffin et al., 1991). Radii of the outer boundary of the brain, skull and scalp region equal to 8 cm, 8.5 cm and 9.2 cm, respectively, were used. The dipole coordinates  $x$  (left ear to right ear),  $y$  (posterior to anterior) and  $z$  (up, through the Cz electrode) were  $(-0.5, 0, 0.1)$  relative to the outer radius and the dipole orientations  $dx$ ,  $dy$  and  $dz$  were equal to  $(1, 0, 0)$ . The amplification factors at each electrode were then multiplied with a 5.7-Hz sine wave. Twenty-one electrodes were used according to the 10–20 system for electrode placement (Nuwer et al., 1998) and additional electrodes T1 and T2 on the temporal region. The time course of the scalp potentials was stored in a  $500 \times 21$  dimensional matrix  $\mathbf{A}$ , representing 2 s of EEG with sample frequency of 250 Hz.

A  $500 \times 21$  noise matrix  $\mathbf{B}$  contained 2 s of awake background EEG activity, recorded with the same electrode configuration, from a normal subject. On this matrix  $\mathbf{B}$ , muscle artifacts were superimposed. These muscle artifacts were separated from contaminated background activity using BSS-CCA (De Clercq et al., 2006). In the simulation study, the noise matrix  $\mathbf{B}$  was superimposed on the signal matrix  $\mathbf{A}$  containing the epileptical activity:

$$\mathbf{X}(\lambda) = \mathbf{A} + \lambda \cdot \mathbf{B}$$

with  $\lambda \in \mathbb{R}$  (Fig. 4B). The data were digitally filtered by a band-pass filter (0.3–35 Hz). The root mean squared (RMS) value of the signal with  $N$  data points and  $S$  channels is then equal to

$$\text{RMS}(\mathbf{A}) = \sqrt{\frac{1}{S \cdot N} \sum_{s=1}^S \sum_{n=0}^{N-1} (\mathbf{A}(n, s))^2}$$

and the RMS value of the noise is equal to

$$\text{RMS}(\lambda \cdot \mathbf{B}) = \sqrt{\frac{1}{S \cdot N} \sum_{s=1}^S \sum_{n=0}^{N-1} (\lambda \cdot \mathbf{B}(n, s))^2}$$

An important measure was the signal-to-noise ratio (SNR) which is defined as follows,

$$\text{SNR} = \frac{\text{RMS}(\mathbf{A})}{\text{RMS}(\lambda \cdot \mathbf{B})}$$

Changing the parameter  $\lambda$  alters the noise level of the simulated signal. We performed several simulations with different noise levels. The aim of this simulation study was to evaluate the

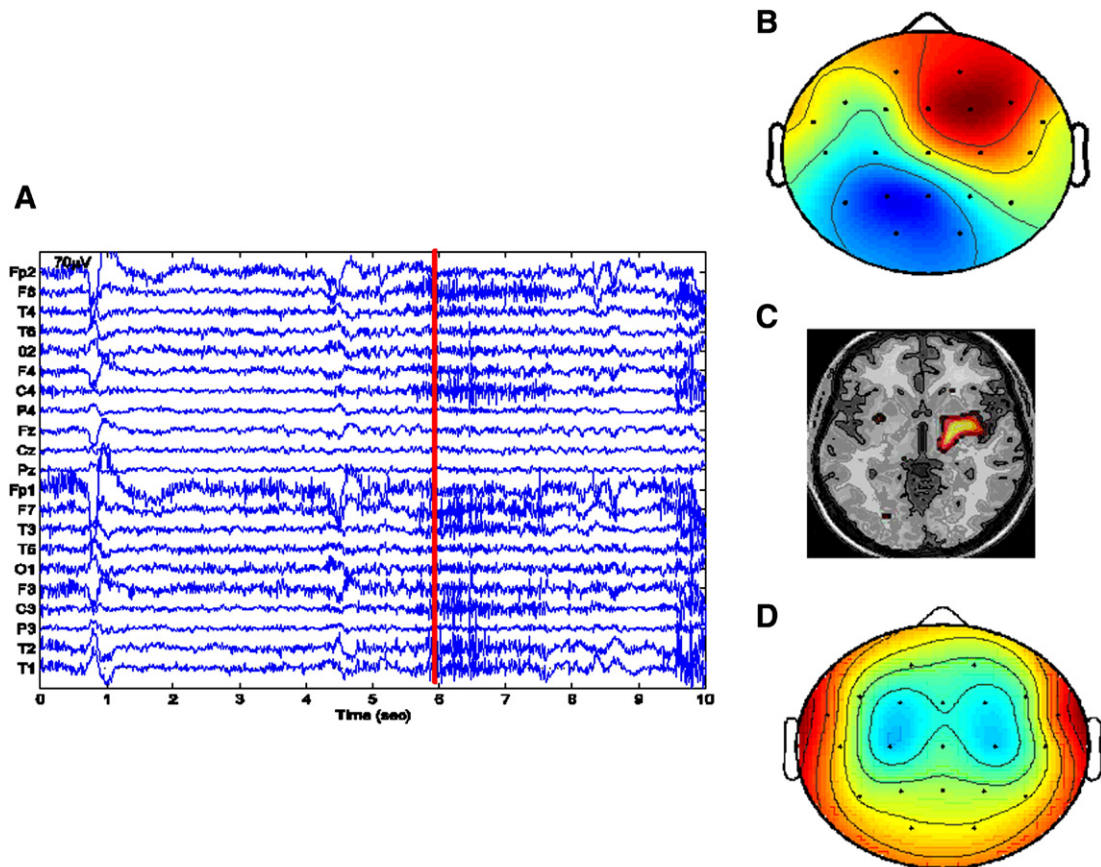


Fig. 6. (A) 10-s of EEG during a seizure without clear ictal EEG changes, the red line indicates the start of the 2-s used in the CP analysis. (B) The spatial distribution of the epileptic atom (red area) and (C) SISCOM. The spatial distribution of the identified atom was concordant with SISCOM. (D) The first singular vector was not informative.

performance of the proposed method in extracting the potential distribution of the 4-Hz epileptiform activity, for different noise levels. The performance was evaluated by the correlation coefficient between the true potential distribution and the extracted potential distribution of the seizure activity (Fig. 4C). We compared this performance with results obtained with the CP method on the power of wavelet transformed EEG, as is described in previous publications. We also compare our method with the localizing information that can be obtained from the SVD. We compare our results with the first left singular vector (Fig. 4C).

#### Clinical validation on ictal EEGs

##### EEG acquisition

Video-EEGs were recorded on 21-channel OSG EEG recorders (Rumst, Belgium). Electrodes were placed according to the International 10–20 System with additional sphenoidal electrodes. Sampling frequency was 250 Hz and an average reference montage was used. The EEG was digitally filtered by a band-pass filter (0.3–35 Hz). A notch filter was applied to suppress the 50-Hz power line interference.

##### Data selection

Patients, who underwent a full presurgical evaluation for refractory partial epilepsy, were included when seizure semeiology,

structural MRI, interictal EEG, subtraction ictal SPECT co-registered with MRI (SISCOM) and neuropsychological assessment were concordant and reliably defined the epileptogenic zone. Ictal EEG findings were not an inclusion criterion. SISCOM that was concordant with other data was a selection criterion. SISCOM was considered the gold standard with which we compared the localization of ictal EEG as determined by visual assessment and the CP decomposition method. SISCOM images were displayed on a standard MRI in MNI (Montreal Neurological Institute) space using a minimum threshold of  $z=2$  (for details on this procedure, see Nelissen et al., 2006). An epileptologist, who was aware of all the data of the presurgical evaluation, selected the ictal EEG recordings. The selected EEG was of the seizure during which the ictal SPECT injection was given. One ictal EEG per patient was used in this study. Thirty-seven EEGs were included in the study. The ictal EEGs were also presented to a clinical neurophysiologist/epileptologist, who was blinded to all other clinical and localizing data, for visual assessment of the ictal EEGs and determination of the localization and lateralization of the ictal onset. The validation study is performed on the same data set as described in Vergult et al. (2007). In this paper, all details concerning the optimal conditions under which visual reading was performed are described (e.g. band-pass filtering as well as the amplitude could be freely adjusted by the human reader). Localization of ictal EEG (both visual assessment and CP method) was considered correct when lobe of onset was concordant with SISCOM findings.

Thirty-seven patients fulfilled the inclusion criteria. Twenty-four were women. Median age was 33 years (range: 14–62). Median age at seizure onset was 14 years (0–62). The median seizure frequency per month was 6 (1–600). MRI showed unilateral hippocampal sclerosis ( $n=10$ ), focal cortical dysplasia ( $n=5$ ), scar tissue ( $n=5$ ), a tumor ( $n=3$ ), dual pathology ( $n=2$ ), a cavernous angioma ( $n=1$ ) or no abnormality ( $n=10$ ). Seventeen patients underwent an operation. With a follow-up of more than 2 years, 12 have remained seizure free and 5 almost seizure free. Five patients refused surgery, and 15 were not offered surgery, because the epileptogenic zone involved eloquent cortex ( $n=6$ ) or the MRI did not reveal an abnormality ( $n=9$ ).

The ictal SPECT injection was given during a complex partial seizure ( $n=32$ ), simple partial seizure ( $n=2$ ) or secondarily generalized seizure ( $n=3$ ). The median duration of the injected seizure was 70 s (range: 11–389) and the median time of injection was 26 s after seizure onset (range: 3–109).

### Statistics

In order to estimate the statistical significance of the improvement of this automatic localization compared with blinded human reading, a non-parametric signed rank test was performed.

## Results

### Simulation study

The correlation between the simulated distribution and the spatial distribution in the simulation study, extracted with the CP method, is shown in Fig. 4C. The figure shows that the CP method correctly localized epileptic activity despite severe contamination with noise. One can expect that a real seizure EEG has an SNR much larger than 0.42. But even at this low noise level (Fig. 4B), the correct potential distribution is extracted.

The figure also shows that pure wavelet-transformed EEG, which we used, was better than the decomposition on the power of the wavelet-transformed EEG as it was described in previous publications.

A comparison of the localizing value of the CP method and the SVD on the same simulated data is also given in Fig. 4C. Adding frequency information and decomposing the array in a unique, unconstrained way clearly improves localization.

### Clinical validation

The CP method correctly localized the seizure onset zone in 34 of 37 cases (92%) while a human reader, blinded to all other information, was able to localize 21 of 37 cases (57%). This improvement is significant ( $p=0.00024$ ). From 3 EEGs no automatic localization could be obtained. In one seizure, there was an electrode artifact during the whole seizure, which impeded a reliable decomposition. Two spatial distributions did not clearly reveal the epileptical focus because there were high potentials at both sides of the brain, which indicates that no perfect separation of ictal activity from background EEG was obtained with the CP decomposition. Localization can only be derived when all the active electrodes are adjacent. Otherwise the decomposition is not meaningful. The human reader did not recognize ictal activity in 3 cases, was not able to localize the seizure onset in 7 cases and wrongly localized the seizure onset in 6 cases. Figs. 5–7 illustrate our results with 3 cases. Fig. 5A shows a 10-s epoch of EEG with the

beginning of a frontal lobe seizure in the last 2 s, that could not be localized by visual inspection of the EEG. However, the CP method localization (Fig. 5B), obtained with 2 s of EEG starting from the red line, was concordant with the SISCOM findings (Fig. 5C). Fig. 5D shows the first left singular vector, which does not provide a clear localization. Fig. 5E1–2 show the atoms of the decomposition of the same EEG when the power of the wavelet-transformed EEG was used in the decomposition. None of the images revealed the epileptic focus. The figure illustrates that the pure wavelet transformed EEG is much less influenced by the muscle artifacts than the power of the wavelet transformed EEG. When computing the power, the underlying structure is not trilinear anymore.

Fig. 6 illustrates the sensitivity of the CP method: the ictal activity was not visible on visual assessment of the EEG, while the decomposition findings were concordant with SISCOM.

Fig. 7 shows the data of a patient with a right posterior focus, which was not detected with the CP method using a time window of 2 s due to the rhythmic eye artifacts. When removing the eye artifacts, or computing the decomposition between 2 eye blinks, the correct focus was obtained (Fig. 7B). The SVD detected remaining eye artifacts (Fig. 7D1) and did not reveal the focus in other singular vectors (Fig. 7D2).

## Discussion

In this paper, we introduced a new method for extracting the potential distribution of ictal EEG activity, which is a novel, fast and sensitive method to visualize the ictal onset zone. The method is based on the multi-way CP decomposition of wavelet-transformed EEG in distinct ‘atoms’. After the decomposition, one atom can be identified as the epileptical atom, and the spatial component of this atom reveals the focus. To the best of our knowledge, we are the first to propose a decomposition method that separates ictal activity from background EEG into one component. We claim that the CP method exploits the fact that seizure activity remains more localized in space and frequency during a short time interval than background EEG signals. The components in the CP decomposition should model most of the variation of the array, i.e. model the dominant activity. This modeled activity will be a signal with high amplitudes or a signal with stable components in frequency and spatial distribution. The background EEG and random noise (e.g. muscle artifacts) cannot be modeled with this simple CP structure and the CP decomposition will be insensitive to such random artifacts. This is an advantage, as there is no need to first remove these artifacts. All EEG signals that cannot be modeled contribute to the residuals  $e_{ijk}$ .

Seizure activity is often obscured by artifacts, which complicates visual analysis. These artifacts can be removed with different techniques (see e.g. Urrestarazu et al., 2004; Delorme et al., 2007, and references herein). Our BSS-CCA method for muscle artifact removal made visual analysis of ictal EEG more sensitive (Vergult et al., 2007). Our current CP method is also more sensitive than visual assessment, with the additional advantage that the technique is automatic and more objective, i.e. not dependent on a subjective visual interpretation. By means of simulations, we showed that the method is able to extract the correct potential distribution, even at very low SNRs. The validation study demonstrated that the method may be a valuable and objective localizing tool for the epileptologist in clinical practice.

As opposed to, e.g., Miwakeichi et al. (2004), who used the complex wavelet to obtain a 3D tensor, we used a real wavelet. In



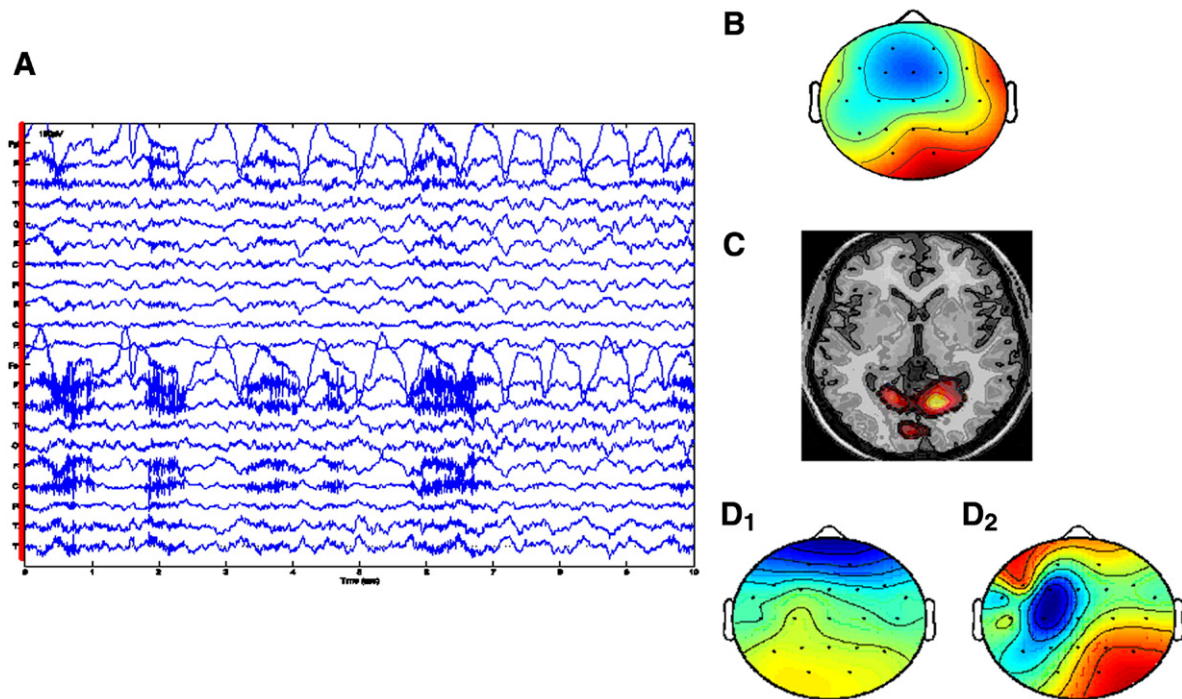


Fig. 7. (A) 10-s EEG recording of a right occipital seizure showed frequent eye blinks (Fp1 and Fp2), but no clear ictal activity, the red line indicates the start of the 2-s used in the CP analysis. (B) The spatial distribution of the epileptical atom and (C) SISCOM showed a concordant focus in the right occipital lobe. (D1–2) Two singular vectors did not give clear localizing information.

addition, we did not decompose the power of the wavelet-transformed EEG. We demonstrated that by decomposing ‘pure’ wavelet-transformed EEG, the method became very robust for muscle artifacts and low SNRs because random ‘noise’ cannot be modeled with this restricted CP model.

We have used SISCOM as a gold standard for the ictal onset zone. It is well known that the time resolution of ictal SPECT is poor and that areas of hyperperfusion often represent a combination of ictal onset zone and propagated activity, even when ictal SPECT injections were given early during a seizure. Selection of patients who were rendered seizure free after surgery would have made our sample size rather small. Since the aim of the present study was to compare the sensitivity of two methods of analysis of the same EEG data set (visual analysis versus CP method) to detect the ictal onset zone, we believe that our current inclusion criteria were sufficient to reliably indicate the lobe of seizure onset.

In our study, we have compared 2D data of the CP method with 3D data of ictal SPECT in a qualitative fashion. We are currently working on a method to display the extracted potential distributions of the CP method in 3D, which could be co-registered with MRI and subtracted ictal SPECT. Nowadays, dipole modeling or other source localization techniques can rarely be applied to ictal EEGs, because the EEGs are too much contaminated by artifacts. The advantage of the extraction of the whole potential distribution of the epileptical activity in one component opens perspectives for source localization techniques of seizure onset activity in all patients. This would be an extension of the work done by other groups about source localization after signal decomposition (see e.g. Kobayashi et al., 2002a,b). It would open the way for a multimodality imaging platform in which the epileptic lesion is displayed together with two methods to localize the ictal onset zone, namely ictal SPECT and the ictal onset zone detected by

canonical decomposition of the ictal scalp EEG, which is routinely and easily obtained during long-term video-EEG monitoring.

The length of the time window in which a CP decomposition is computed is not a critical issue as long as the seizure activity remains well localized. When analyzing a seizure, it is important that the CP decomposition is computed in a time window at the seizure onset in order to localize seizure onset zone. It will be interesting to compute different decompositions with a short time window at consecutive time points during a seizure. Each decomposition will have localizing information for the considered time interval and may highlight seizure propagation patterns. Our CP method could be important in the presurgical evaluation of frontal lobe seizures that are characterized by fast propagation and ictal EEGs that are difficult to interpret on visual assessment. Because of potential fast propagation, we used a time window of 2 s in our study, which is probably the smallest window in which our algorithm will give reliable information. We postulate that our CP method, with high temporal resolution, may improve the interpretation of SISCOM, which has an excellent spatial resolution but notoriously poor temporal resolution (i.e. it shows a combination of ictal onset zone and seizure propagation pathways).

Currently, we are working on a reliable implementation of the inverse continuous wavelet transform in order to reconstruct the ictal atom in the standard EEG matrix. When this is possible, the clinician will be able to look at the seizure activity on EEG, separated from artifacts and background signal.

The aim of epilepsy surgery is the complete resection or complete disconnection of the epileptogenic zone, which is defined as the area of cortex indispensable for the generation of clinical seizures. We use a variety of diagnostic tools, such as analysis of seizure semiology, EEG recordings, functional testing and

neuroimaging techniques to define the location and boundaries of the epileptogenic zone. It should be stressed that a priori knowledge of the exact timing of the clinical seizure was essential in the application of our algorithm, i.e. it is not a seizure detection algorithm. We showed that our algorithm was more sensitive in the delineation of the ictal onset zone than visual assessment of the ictal EEG according to current standards. The exact relationship, however, between ‘activated electrodes’ using our algorithm and the ictal process in the brain will need further validation studies. We plan to do this with correlation studies between a 3D version of our algorithm and ictal SPECT, simultaneously recorded depth EEG studies, and ictal EEGs of patients with an established epileptogenic zone, i.e. patients who were rendered seizure free after epilepsy surgery. The spatial resolution of our methodology could be improved using high density array EEG studies.

In this study, we only evaluated one EEG recording from each patient. It will be interesting to analyze all seizures recorded from the same patient during a presurgical evaluation using our CP method. When all epileptical potential distributions obtained with the CP decomposition at seizure onset are very similar, it can be expected that there is only one epileptogenic focus. However, when different distributions are obtained, there might be different foci and surgery may not be a good option. Although this is current practice in the presurgical evaluation of patients with refractory partial epilepsy, we anticipate that the higher sensitivity of our CP method as compared with visual assessment of the ictal EEGs will improve and streamline the non-invasive presurgical evaluation of patients with refractory partial epilepsy.

## Acknowledgments

The figures shown in this paper are made with EEGLAB (Delorme and Makeig, 2004).

We would like to thank Guido Van Driel for helpful discussions on epilepsy and EEG.

This research is funded by a PhD grant of the Institute for the Promotion of Innovation through Science and Technology in Flanders (IWT-Vlaanderen).

Research supported by Research Council KUL: GOA-AMBioRICS, CoE EF/05/006 Optimization in Engineering, IDO 05/010 EEG-fMRI, several PhD/postdoc and fellow grants; Flemish Government: FWO: PhD/postdoc grants, projects, G.0407.02 (support vector machines), G.0360.05 (EEG, Epileptic), G.0519.06 (Non-invasive brain oxygenation), FWO-G.0321.06 (Tensors/Spectral Analysis), G.0341.07 (Data fusion), research communities (ICCoS, ANMMM); IWT: PhD Grants; Belgian Federal Science Policy Office IUAP P5/22 (‘Dynamical Systems and Control: Computation, Identification and Modelling’); EU: BIOPATTERN (FP6-2002-IST 508803), ETUMOUR (FP6-2002-LIFESCIHEALTH 503094), Healthagents (IST-2004-27214, FAST (FP6-MC-RTN-035801); ESA: Cardiovascular Control (Prodex-8 C90242).

## References

- Acar, E., Bingol, C.A., Bingol, H., Yener, B. Computational analysis of epileptic focus localization, Proc. of The Fourth IASTED International Conference on Biomedical Engineering (BIOMED-2006).
- Carroll, J.D., Chang, J., 1970. Analysis of individual differences in multidimensional scaling via an n-way generalization of ‘Eckart–Young’ decomposition. *Psychometrika* 35, 283–319.
- Cuffin, B.N., Cohen, D., Ynokuchi, K., Maniewski, R., Purcell, C., Cosgrove, G.R., Ives, J., Kennedy, J., Schomer, D., 1991. Tests of EEG localization accuracy using implanted sources in the human brain. *Ann. Neurol.* 29, 132–138.
- De Clercq, W., Vergult, A., Vanrumste, B., Van Paesschen, W., Van Huffel, S., 2006. Canonical correlation analysis applied to remove muscle artifacts from the encephalogram. *IEEE Trans. Biomed. Eng.* 53, 2583–2587.
- De Lathauwer, L., 2006. A link between the canonical decomposition in multilinear algebra and simultaneous matrix diagonalization. *SIAM J. Matrix Anal. Appl.* 28, 642–666.
- De Lathauwer, L., De Moor, B., Vandewalle, J., 2000. A multilinear singular value decomposition. *SIAM J. Matrix Anal. Appl.* 21, 1253–1278.
- De Lathauwer, L., De Moor, B., Vandewalle, J., 2004. Computation of the canonical decomposition by means of a simultaneous generalized Schur decomposition. *SIAM J. Matrix Anal. Appl.* 26, 295–327.
- Delorme, A., Makeig, S., 2004. EEGLAB: an open source toolbox for analysis of single-trial EEG dynamics. *J. Neurosci. Methods* 134, 9–21.
- Delorme, A., Sejnowski, T., Makeig, S., 2007. Enhanced detection of artifacts in EEG data using higher-order statistics and independent component analysis. *NeuroImage* 34, 1443–1449.
- Dietsch, G., 1932. Fourier-analyse van elektroencephalogrammen des menschen. *Pflügers Arch. Gesamte Physiol.* 230, 106–112.
- Foldvary, N., Klem, G., Hammel, J., Bingaman, W., Najm, I., Lüders, H., 2001. The localizing value of ictal EEG in focal epilepsy. *Neurology* 57, 2022–2028.
- Gotman, J., 1982. Automatic recognition of epileptic seizures. *Electroencephalogr. Clin. Neurophysiol.* 54, 530–540.
- Gotman, J., 2003. Noninvasive methods for evaluating the localization and propagation of epileptic activity. *Epilepsia* 44, 21–29.
- Harshman, R.A., 1970. Foundations of the CP procedure: models and conditions for an ‘explanatory’ multi-modal factor analysis. UCLA Work. Pap. Phon. 16.
- Hitchcock, F.L., 1927. The expression of a tensor or a polyadic as a sum of products. *J. Math. Phys.* 6, 164–189.
- Kobayashi, K., Akiyama, T., Nakahori, T., Yoshinaga, H., Gotman, J., 2002a. Systematic source estimation of spikes by a combination of independent component analysis and RAP-MUSIC. I: principles and simulation study. *Clin. Neurophysiol.* 113, 713–724.
- Kobayashi, K., Akiyama, T., Nakahori, T., Yoshinaga, H., Gotman, J., 2002b. Systematic source estimation of spikes by a combination of independent component analysis and RAP-MUSIC. II: preliminary clinical application. *Clin. Neurophysiol.* 113, 725–734.
- Kobayashi, K., Yoshinaga, H., Ohtsuka, Y., Gotman, J., 2005. Dipole modeling of epileptic spikes can be accurate or misleading. *Epilepsia* 46, 397–408.
- Kruskal, J.B., 1977. Three-way arrays: rank and uniqueness of trilinear decompositions, with applications to arithmetic complexity and statistics. *Psychometrika* 18, 95–138.
- LeVan, P., Urrestarazu, P., Gotman, J., 2006. A system for automatic artifact removal in ictal scalp EEG based on independent component analysis and Bayesian classification. *Clin. Neurophysiol.* 117, 912–927.
- Miwauchi, F., Martinez-Montes, E., Valdés-Sosa, P.A., Nishiyama, N., Mizuhara, H., Yamaguchi, Y., 2004. Decomposing EEG data into space–time–frequency components using parallel factor analysis. *NeuroImage* 22, 1035–1045.
- Morup, M., Hansen, L.K., Herrmann, C.H.S., Parnas, J., Arnfred, S.M., 2006. Parallel factor analysis as an exploratory tool for wavelet transformed event-related EEG. *NeuroImage* 29, 938–947.
- Nelissen, N., Van Paesschen, W., Baete, K., Van Laere, K., Palmmini, A., Van Billoen, H., Dupont, P., 2006. Correlations of interictal FDG-PET metabolism and ictal SPECT perfusion changes in human temporal lobe epilepsy with hippocampal sclerosis. *NeuroImage* 32, 684–695.
- Niedermeyer, E., 1987. Epileptic seizure disorder, In: Niedermeyer, E., Lopes da Silva, F. (Eds.), *Electroencephalography: Basic Principles, Clinical Applications and Related Fields*, second edition. Urban and Schwarzenberg, Baltimore. Chapter 27.

- Nuwer, M.R., Comi, G., Emmerson, R., Fuglsang-Frederiksen, A., Guerit, J.M., Hinrichs, H., Ikeda, A., Luccas, F.J., Rappelsberger, P., 1998. IFCN standards for digital recording of clinical EEG. *Electroencephalogr. Clin. Neurophysiol.* 106, 259–261.
- Oostendorp, T.F., Delbeke, J., Stegeman, D.F., 2000. The conductivity of the human skull: results of in vivo measurements. *IEEE Trans. Biomed. Eng.* 47, 1487–1492.
- Rosenow, F., Lüders, H., 2001. Presurgical evaluation of epilepsy. *Brain* 124, 1683–1700.
- Salu, Y., Cohen, L.G., Rose, D., Sato, S., Kufta, C., Hallett, M., 1990. An improved method for localizing electric brain dipoles. *IEEE Transactions on Biomedical Engineering* 37, 699–708.
- Scherg, M., von Cramon, D., 1985. Two bilateral sources of the late AEP as identified by a spatio-temporal dipole model. *Electroencephalography and Clinical Neurophysiology* 62, 32–44.
- Sidiropoulos, N.D., Bro, R., 2000. On the uniqueness of multilinear decomposition of N-way arrays. *J. Chemom.* 14, 229–239.
- Smilde, A., Bro, R., Geladi, P., 2004. *Multivariate Analysis with Applications in the Chemical Sciences*. John Wiley and Sons.
- Spencer, S.S., Williamson, P.D., Briders, S.L., Mattson, R.H., Cicchetti, D.V., Spencer, D.D., 1985. Reliability and accuracy of localization by scalp ictal EEG. *Neurology* 30, 1567–1575.
- Stegeman, A., Sidiropoulos, N.D., 2007. On Kruskal's uniqueness condition for the Candecomp/Parafac decomposition. *Lin. Alg. Appl.* 420, 540–552.
- Tang, A.C., Sutherland, M.T., McKinney, C.h.J., 2004. Validation of sobi components from high-density EEG. *NeuroImage* 25, 539–553.
- Tucker, L., 1964. The extension of factor analysis to three-dimensional matrices. In: Frederiksen, N., Gulliksen, H. (Eds.), *Contributions to Mathematical Psychology*. Holt, Rinehart Winston, New York, pp. 110–182.
- Tucker, L., 1966. Some mathematical notes on three-mode factor analysis. *Psychometrika* 31, 279–311.
- Urrestarazu, E., Iriarte, J., Alegre, M., Valencia, M., Viteri, C., Artieda, J., 2004. Independent component analysis removing artifacts in ictal recordings. *Epilepsia* 45, 1071–1078.
- Vergult, A., De Clercq, W., Palmieri, A., Vanrumste, B., Dupont, P., Van Huffel, S., Van Paesschen, W., 2007. Improving the interpretation of ictal scalp EEG: BSS-CCA algorithm for muscle artifact removal. *Epilepsia* 48, 550–558.